Overcoming GNSS Degradation by Cooperative Networked Localization of Autonomous Vehicles

Mattia Brambilla[1], Domenico Gaglione[2], Giovanni Soldi[2], Leonardo Millefiori[2], Monica Nicoli[1], and Paolo Braca[2]

[1]Politecnico di Milano, Milan, Italy
[2]NATO STO Centre for Maritime Research and Experimentation (CMRE), La Spezia, Italy

Abstract

This paper addresses the problems of cooperative localization and multi-target tracking in a network of mobile vehicles sensing an unknown number of targets. Mobility and uncertainty on the target existence make the localization problem complex as vehicles have to first perform a cooperative self localization for network positioning, and then carry out a multi-target tracking algorithm. These two tasks are here merged in one framework that models the complete network as a time variant factor graph, which is used as baseline to perform message passing algorithm. The proposed methodology is given in a general formulation, thus being able to account for any multistatic network configuration, with multiple transmitters and receivers. The validation phase is carried out in a simulated urban environment and in a real maritime surveillance use case with a dataset collected by NATO STO CMRE.

1 Introduction

Localizing unknown objects (i.e. targets) from moving sensors is a challenging task which requires an accurate knowledge of the position of the vehicles carrying the sensing devices. The localization of these sensing vehicles can be performed with technologies and techniques that are specific to the application. In land, air, and maritime (above water) domains, global navigation satellite system (GNSS) is widely acknowledged as primary localization technology which, in its several implementations — e.g., global navigation system (GPS), Galileo, GLONASS — has been used for decades for both military and civil applications [1]. However, GNSS coverage, integrity and accuracy can be jeopardized during operations — leading to unreliable and incoherent positioning information — as a result of communication failures, hardware malfunctioning, or undesired external attacks (e.g. jamming and spoofing), the latter being a serious threat especially for military and defense-related applications. Overcoming the GNSS unavailability to provide seamless accurate localization becomes a priority in case of time-and-safety-critical use cases. An intuitive, yet useful, mitigation approach is to adopt multiple complementary sensing technologies operating over different hardware systems, frequencies and, possibly, places of installations, along with the use of communication technologies enabling multi-vehicle cooperation.

Cooperative techniques have been demonstrated to enhance the localization performance of an individual sensor, with increased situational awareness and environment reconstruction in indoor/outdoor scenarios, for civil/military applications, and industrial/domestic needs [2–11]. Multi-sensor systems are extremely common in case of static network geometry [12–14], but the use of mobile sensors introduces the possibility to design optimal trajectories for more accurate target localization [15].

This work was supported in part by the NATO Allied Command Transformation (ACT) under the DKOE project.

This paper proposes an algorithm for cooperative self-localization that overcomes GNSS availability by exploiting both inter-vehicle communications and information obtained from the estimation of the position of detected targets, either stationary (e.g., anchor points) or moving. The combination of cooperative self-localization (CSL) of vehicles and multi-target tracking (MTT) in one unique solution is addressed by making use of the sum-product algorithm, a message passing algorithm working on a suitable devised factor graph [16]. The proposed methodology operates in a centralized setting, meaning that data collected across multiple vehicles are sent towards a single control center, which is in charge of performing all the required processing for localization of both vehicles and targets; nevertheless, extension to a fully distributed approach is possible by proper adaptation (e.g., by combination with consensus [19]). The proposed methodology poses its fundamentals on state-of-the-art literature [12–14, 16–22], and contributes to scientific knowledge by incorporating a truly-defined MTT problem — that accounts for clutter measurements (i.e., false alarms), missed detections, target (dis)appearance and intermittent measurement availability — into the CSL of mobile vehicles.

The reminder of the paper is organized as follows. Section 2 presents the system model with the definition of vehicles, targets and associated measurements. Section 3 is used to formulate the CSL and MTT problem with focus on the derivation of the joint posterior pdf. Section 4 presents numerical results in an urban scenario as well as in a maritime experimentation. Section 5 draws conclusions of this work.

2 System model

2.1 Vehicles and potential targets

Let us consider a set $\mathcal{V} \triangleq \{1, \dots, V\}$ of vehicles with known cardinality V. Vector $\boldsymbol{s}_{a,t}$ defines the state (e.g., position and velocity) of vehicle $a \in \mathcal{V}$ at time t, and its evolution in time is modeled as

$$\boldsymbol{s}_{a,t} = \boldsymbol{\varepsilon}(\boldsymbol{s}_{a,t-1}, \boldsymbol{u}_{a,t}), \tag{1}$$

where $\boldsymbol{u}_{a,t}$ is a driving process. The function $\boldsymbol{\varepsilon}(\cdot)$ and the statistics of $\boldsymbol{u}_{a,t}$ define the vehicle state transition pdf $f(\boldsymbol{s}_{a,t}|\boldsymbol{s}_{a,t-1})$. We denote the joint vehicle state vector at time t as $\boldsymbol{s}_t \triangleq [\boldsymbol{s}_{1,t}^{\mathsf{T}}, \dots, \boldsymbol{s}_{V,t}^{\mathsf{T}}]^{\mathsf{T}}$, and the joint vehicle state vector at all times as $\boldsymbol{s}_{1:t} \triangleq [\boldsymbol{s}_1^{\mathsf{T}}, \dots, \boldsymbol{s}_t^{\mathsf{T}}]^{\mathsf{T}}$. A vehicle is supposed to be equipped with transmission and/or reception hardware (with limited range, in general), allowing to collect and share measurements. We indicate with $\mathcal{T} \subseteq \mathcal{V}$ the set of vehicles equipped with a transmitter (Tx-vehicles), and with $\mathcal{R} \subseteq \mathcal{V}$ the set of vehicles equipped with a receiver (Rx-vehicles), such that $\mathcal{T} \cup \mathcal{R} = \mathcal{V}$; note that the set $\mathcal{T} \cap \mathcal{R}$ might not be empty, and represents the set of vehicles equipped with both a transmitter and a receiver. If $|\mathcal{T}| = 1$ and $|\mathcal{R}| \geqslant 1$ the network configuration is referred to as bistatic, otherwise when $|\mathcal{T}| > 1$ and $|\mathcal{R}| \geqslant 1$ it is referred to as multistatic.

To account for the time-varying and unknown number of targets, we use the notion of potential target (PT) introduced in [13]. Let K_t be the number of PTs at time t, which is the maximum possible number of targets that have been detected up to time t, and let $\mathcal{K}_t \triangleq \{1, \dots, K_t\}$ be the set of these PTs. We indicate with $\boldsymbol{x}_{k,t}$ and $r_{k,t} \in \{0, 1\}$, respectively, the state and existence of PT $k \in \mathcal{K}_t$ at time t, and with $\boldsymbol{y}_{k,t} \triangleq [\boldsymbol{x}_{k,t}^{\mathsf{T}}, r_{k,t}]^{\mathsf{T}}$ its augmented state.

2.2 Measurements

At any time t, vehicle $a \in \mathcal{V}$ might have several types of measurements — i.e., observations of any vehicle state $\boldsymbol{s}_{a,t}$, even its own state, and PT state $\boldsymbol{x}_{k,t}$ — available to perform CSL and MTT. We distinguish between measurements with *unknown* origins and measurements with *known* origins. For the former, it is unknown if they generated from clutter, from vehicles, or from PTs, and, in the latter two cases, also from which vehicles or PTs; this thus requires to consider all the possible combinations of measurements and vehicles or PTs, known as data association (DA). Measurements with known origins, instead, are unambiguous and do not require any DA.

Among the measurements with known origins, we consider navigation measurements and inter-vehicle measurements. The navigation measurement $\boldsymbol{g}_{a,t}$ is an observation made by vehicle $a \in \mathcal{V}_t^g \subseteq \mathcal{V}$ of its own state $\boldsymbol{s}_{a,t}$,

Note that the state $\boldsymbol{x}_{k,t}$ of PT k is formally considered also if $r_{k,t} = 0$.

and modeled as

$$\boldsymbol{g}_{a,t} = \boldsymbol{\theta}_a\big(\boldsymbol{s}_{a,t}, \boldsymbol{n}_{a,t}\big), \tag{2}$$

where $\boldsymbol{n}_{a,t}$ is a noise term, independent across a and t, modeling the finite accuracy of the measuring on-board system, e.g., GPS receiver; the function $\boldsymbol{\theta}_a(\cdot)$ and the statistics of $\boldsymbol{n}_{a,t}$ define the likelihood function $\mathfrak{g}_a(\boldsymbol{g}_{a,t}|\boldsymbol{s}_{a,t})$. We indicate with $\mathcal{V}_t^g$ the set of vehicles that have a navigation measurement available at time t. We introduce the stacked vector of all navigation measurements at time t from all the vehicles $a \in \mathcal{V}_t^g$ as $\boldsymbol{g}_t$, and the stacked vector of all navigation measurements at all times as $\boldsymbol{g}_{1:t} \triangleq [\boldsymbol{g}_1^\mathsf{T}, \ldots, \boldsymbol{g}_t^\mathsf{T}]^\mathsf{T}$. The inter-vehicle measurement $\boldsymbol{\rho}_t^{(a,a')}$ is an observation, made by the Rx-vehicle $a \in \mathcal{R}$, of the state $\boldsymbol{s}_{a',t}$ of the Tx-vehicle $a' \in \mathcal{T} \setminus \{a\}$, modeled as

$$\boldsymbol{\rho}_t^{(a,a')} = \boldsymbol{\vartheta}\big(\boldsymbol{s}_{a,t}, \boldsymbol{s}_{a',t}, \boldsymbol{w}_t^{(a,a')}\big), \tag{3}$$

where $\boldsymbol{w}_t^{(a,a')}$ is a noise term independent and identically distributed across a, a', and t. The function $\boldsymbol{\vartheta}(\cdot)$ and the statistics of $\boldsymbol{w}_t^{(a,a')}$ define the likelihood function $\mathfrak{d}(\boldsymbol{\rho}_t^{(a,a')}|\boldsymbol{s}_{a,t}, \boldsymbol{s}_{a',t})$. For convenience, we introduce the following sets: the set of Tx-vehicles that provide an inter-vehicle measurement to Rx-vehicle a at time t as $\mathcal{T}_t^{(a)} \subseteq \mathcal{T} \setminus \{a\}$, and the set of Rx-vehicles that receive an inter-vehicle measurement from Tx-vehicle a' at time t as $\mathcal{R}_t^{(a')} \subseteq \mathcal{R} \setminus \{a'\}$. Moreover, we define the stacked vector of all inter-vehicle measurements at Rx-vehicle $a \in \mathcal{R}$ at time t as $\boldsymbol{\rho}_t^{(a)}$, the stacked vector of all inter-vehicles measurements at all Rx-vehicles at time t as $\boldsymbol{\rho}_t$, and the stacked vector of all inter-vehicles measurements at all Rx-vehicles at all times as $\boldsymbol{\rho}_{1:t} = [\boldsymbol{\rho}_1^\mathsf{T}, \ldots, \boldsymbol{\rho}_t^\mathsf{T}]^\mathsf{T}$.

Measurements with unknown origins are those obtained through a detection process. Let us assume that Tx-vehicle $a \in \mathcal{T}$ broadcasts a signal that, before being received by Rx-vehicle $a' \in \mathcal{R}$, is reflected by an object, either a vehicle $a'' \in \mathcal{V} \setminus \{a, a'\}$ or a PT $k \in \mathcal{K}_t$; Rx-vehicle a' can thus extract a measurement that is an observation of the state of the object that caused the reflection, referred to as multi-object tracking (MOT) measurement. Note that, if Tx-vehicle a and Rx-vehicle a' coincides, i.e., if $a = a'$, the MOT measurement is acquired in a monostatic geometry, otherwise it is acquired in a bistatic geometry; moreover, since the set of MOT measurements is obtained through a detection process, it can be affected by false alarms and missed detections. For convenience, let us consider the Cartesian product set $\mathcal{R} \times \mathcal{T}$ of all the possible pairs (a, a') such that $a \in \mathcal{R}$ and $a' \in \mathcal{T}$, and define the pair $j = (a, a')$. The pairs are arbitrarily sorted and define the index set $\mathcal{J} \triangleq \{1, \ldots, J\}$, with $J = |\mathcal{R}||\mathcal{T}|$. Then, assuming that the pair j produces $M_t^{(j)}$ MOT measurements at time t, the m-th MOT measurement can be represented by the vector $\boldsymbol{z}_{m,t}^{(j)}$, $m \in \mathcal{M}_t^{(j)} \triangleq \{1, \ldots, M_t^{(j)}\}$. We follow a sequential approach iterating over the pairs, meaning that the full set of MOT measurements at pair j at time t is processed only if all MOT measurements at previous pair $j' < j$ have already been processed. We introduce the stacked vector of all MOT measurements at pair j at time t as $\boldsymbol{z}_t^{(j)} \triangleq \big[\boldsymbol{z}_{1,t}^{(j)\mathsf{T}}, \ldots, \boldsymbol{z}_{M_t^{(j)},t}^{(j)\mathsf{T}}\big]^\mathsf{T}$, the stacked vector of all MOT measurements at all pairs at time t as $\boldsymbol{z}_t \triangleq [\boldsymbol{z}_t^{(1)\mathsf{T}}, \ldots, \boldsymbol{z}_t^{(J)\mathsf{T}}]^\mathsf{T}$, and the stacked vector of all MOT measurements at all pairs at all times as $\boldsymbol{z}_{1:t} \triangleq [\boldsymbol{z}_1^\mathsf{T}, \ldots, \boldsymbol{z}_t^\mathsf{T}]^\mathsf{T}$. Moreover, we define the vector of numbers of MOT measurements produced at all pairs at time t as $\boldsymbol{m}_t = [M_t^{(1)}, \ldots, M_t^{(J)}]^\mathsf{T}$, and the vector of numbers of MOT measurements produced at all pairs at all times as $\boldsymbol{m}_{1:t} \triangleq [\boldsymbol{m}_1^\mathsf{T}, \ldots, \boldsymbol{m}_t^\mathsf{T}]^\mathsf{T}$.

2.3 Legacy PTs and new PTs

Each PT at time t and pair j is either a "legacy" PT or a "new" PT. A legacy PT represents a survived target, a target that has already been detected either at current time t at any previous pair $j' < j$, or at any previous time $t' < t$. The set of legacy PTs is denoted as $\mathcal{L}_t^{(j)} \triangleq \{1, \ldots, L_t^{(j)}\}$, and their states, existence variables, and augmented states are denoted with $\underline{\boldsymbol{x}}_{\ell,t}^{(j)}$, $\underline{r}_{\ell,t}^{(j)}$, and $\underline{\boldsymbol{y}}_{\ell,t}^{(j)} = [\underline{\boldsymbol{x}}_{\ell,t}^{(j)\mathsf{T}}, \underline{r}_{\ell,t}^{(j)}]^\mathsf{T}$, $\ell \in \mathcal{L}_t^{(j)}$, respectively.

New PTs model those targets that are detected for the first time; one new PT is introduced for each MOT measurement, therefore the number of new PTs at time t and pair j is $M_t^{(j)}$. States, existence variables, and augmented states of new PTs are denoted with $\bar{\boldsymbol{x}}_{m,t}^{(j)}$, $\bar{r}_{m,t}^{(j)}$, and $\bar{\boldsymbol{y}}_{m,t}^{(j)} = [\bar{\boldsymbol{x}}_{m,t}^{(j)\mathsf{T}}, \bar{r}_{m,t}^{(j)}]^\mathsf{T}$, $m \in \mathcal{M}_t^{(j)}$, respectively, where $\bar{r}_{m,t}^{(j)} = 1$ thus means that MOT measurement m was generated by a target that was never detected before (a newly detected target).

Let us define the joint augmented state vectors of legacy PTs and new PTs at time t at pair j as $\underline{\boldsymbol{y}}_t^{(j)} \triangleq [\underline{\boldsymbol{y}}_{1,t}^{(j)\mathsf{T}}, \dots, \underline{\boldsymbol{y}}_{L_t^{(j)},t}^{(j)\mathsf{T}}]^{\mathsf{T}}$ and $\bar{\boldsymbol{y}}_t^{(j)} \triangleq [\bar{\boldsymbol{y}}_{1,t}^{(j)\mathsf{T}}, \dots, \bar{\boldsymbol{y}}_{M_t^{(j)},t}^{(j)\mathsf{T}}]^{\mathsf{T}}$, respectively, and the joint augmented state vector of all new PTs introduced at time t as $\bar{\boldsymbol{y}}_t \triangleq [\bar{\boldsymbol{y}}_t^{(1)\mathsf{T}}, \dots, \bar{\boldsymbol{y}}_t^{(J)\mathsf{T}}]^{\mathsf{T}}$. Note that the vector $\underline{\boldsymbol{y}}_t^{(j)}$ can be interpreted as the vector stacking all the legacy PT augmented states at time t at the previous pair $j-1$, and the new PT augmented states introduced at time t at the previous pair $j-1$, i.e., $\underline{\boldsymbol{y}}_t^{(j)} = [\underline{\boldsymbol{y}}_t^{(j-1)\mathsf{T}}, \bar{\boldsymbol{y}}_t^{(j-1)\mathsf{T}}]^{\mathsf{T}}$. We also introduce the vector $\boldsymbol{y}_t \triangleq [\underline{\boldsymbol{y}}_t^{(1)\mathsf{T}}, \bar{\boldsymbol{y}}_t^{(1)\mathsf{T}}, \bar{\boldsymbol{y}}_t^{(2)\mathsf{T}}, \dots, \bar{\boldsymbol{y}}_t^{(J)\mathsf{T}}]^{\mathsf{T}} = [\underline{\boldsymbol{y}}_t^{(2)\mathsf{T}}, \bar{\boldsymbol{y}}_t^{(2)\mathsf{T}}, \dots, \bar{\boldsymbol{y}}_t^{(J)\mathsf{T}}]^{\mathsf{T}} = \cdots = [\underline{\boldsymbol{y}}_t^{(J)\mathsf{T}}, \bar{\boldsymbol{y}}_t^{(J)\mathsf{T}}]^{\mathsf{T}}$ of all the PT augmented states at time t. The number of PTs at time t, after all the MOT measurements are incorporated, is therefore $K_t \triangleq L_t^{(1)} + \sum_{j=1}^{J} M_t^{(j)} = L_t^{(J)} + M_t^{(J)}$.

3 Problem formulation

The goal is the CSL of vehicles, jointly with the MTT of PTs, to be achieved by combining navigation measurements $\boldsymbol{g}_{1:t}$, inter-vehicle measurements $\boldsymbol{\rho}_{1:t}$, and MOT measurements $\boldsymbol{z}_{1:t}$. The proposed method also aims to improve the localization robustness in case of GNSS navigation unavailability.

We pursue a Bayesian approach that aims to compute the marginal posterior pdfs of all vehicles and PTs, namely $f(\boldsymbol{s}_{a,t}|\boldsymbol{g}_{1:t}, \boldsymbol{\rho}_{1:t}, \boldsymbol{z}_{1:t})$, $\forall a \in \mathcal{V}$, and $f(\boldsymbol{y}_{k,t}|\boldsymbol{g}_{1:t}, \boldsymbol{\rho}_{1:t}, \boldsymbol{z}_{1:t})$, $\forall k \in \mathcal{K}_t$. The state estimates of the vehicles and of the detected PTs (i.e., those for which the marginal posterior existence probability $f(r_{k,t}=1|\boldsymbol{g}_{1:t}, \boldsymbol{\rho}_{1:t}, \boldsymbol{z}_{1:t}) = \int f(\boldsymbol{x}_{k,t}, r_{k,t}=1|\boldsymbol{g}_{1:t}, \boldsymbol{\rho}_{1:t}, \boldsymbol{z}_{1:t}) \mathrm{d}\boldsymbol{x}_{k,t}$ is above a pre-defined threshold P_{ex}) are computed by the minimum mean square error (MMSE) estimator as

$$\hat{\boldsymbol{s}}_{a,t}^{\mathrm{MMSE}} \triangleq \int \boldsymbol{s}_{a,t}\, f(\boldsymbol{s}_{a,t}|\boldsymbol{g}_{1:t}, \boldsymbol{\rho}_{1:t}, \boldsymbol{z}_{1:t})\, \mathrm{d}\boldsymbol{s}_{a,t} \tag{4}$$

and

$$\hat{\boldsymbol{x}}_{k,t}^{\mathrm{MMSE}} \triangleq \int \boldsymbol{x}_{k,t} \frac{f(\boldsymbol{x}_{k,t}, r_{k,t}=1|\boldsymbol{g}_{1:t}, \boldsymbol{\rho}_{1:t}, \boldsymbol{z}_{1:t})}{f(r_{k,t}=1|\boldsymbol{g}_{1:t}, \boldsymbol{\rho}_{1:t}, \boldsymbol{z}_{1:t})}\, \mathrm{d}\boldsymbol{x}_{k,t}\,, \tag{5}$$

respectively. We recall that these state estimates are computed once all the MOT measurements at time t are processed. The pdfs $f(\boldsymbol{s}_{a,t}|\boldsymbol{g}_{1:t}, \boldsymbol{\rho}_{1:t}, \boldsymbol{z}_{1:t})$ and $f(\boldsymbol{y}_{k,t}|\boldsymbol{g}_{1:t}, \boldsymbol{\rho}_{1:t}, \boldsymbol{z}_{1:t})$ are marginal pdfs of the joint posterior pdf $f(\boldsymbol{y}_{0:t}, \boldsymbol{s}_{0:t}, \boldsymbol{\alpha}_{1:t}, \boldsymbol{\beta}_{1:t}|\boldsymbol{g}_{1:t}, \boldsymbol{\rho}_{1:t}, \boldsymbol{z}_{1:t})$ whose expression is provided in the next section, where $\boldsymbol{\alpha}_{1:t}$ and $\boldsymbol{\beta}_{1:t}$ are DA-related variables: they describe the valid associations between the MOT measurements and the vehicles and PTs under the point-target assumption, i.e., the fact that at any time t a vehicle or PT can generate at most one MOT measurement at pair j, and that each MOT measurement $\boldsymbol{z}_{m,t}^{(j)}$ can be generated by at most one vehicle or PT. Note that the DA representation provided by $\boldsymbol{\alpha}_{1:t}$ and $\boldsymbol{\beta}_{1:t}$ is redundant in that $\boldsymbol{\alpha}_{1:t}$ can be obtained by $\boldsymbol{\beta}_{1:t}$ and vice-versa; this redundancy, however, allows us to derive an efficient and scalable algorithm. Details are provided in [13,23].

3.1 Derivation of joint posterior pdf

Given the a-priori pdfs of vehicles and PTs at time $t=0$, namely $f(\boldsymbol{s}_0)$ and $f(\boldsymbol{y}_0)$, the joint posterior pdf $f(\boldsymbol{y}_{0:t}, \boldsymbol{s}_{0:t}, \boldsymbol{\alpha}_{1:t}, \boldsymbol{\beta}_{1:t}|\boldsymbol{g}_{1:t}, \boldsymbol{\rho}_{1:t}, \boldsymbol{z}_{1:t})$ can be computed as

$$\begin{aligned}
&f(\boldsymbol{y}_{0:t}, \boldsymbol{s}_{0:t}, \boldsymbol{\alpha}_{1:t}, \boldsymbol{\beta}_{1:t}|\boldsymbol{g}_{1:t}, \boldsymbol{\rho}_{1:t}, \boldsymbol{z}_{1:t}) \\
&\quad = f(\boldsymbol{y}_{0:t}, \boldsymbol{s}_{0:t}, \boldsymbol{\alpha}_{1:t}, \boldsymbol{\beta}_{1:t}|\boldsymbol{g}_{1:t}, \boldsymbol{\rho}_{1:t}, \boldsymbol{z}_{1:t}, \boldsymbol{m}_{1:t}) \qquad (6)\\
&\quad \propto f(\boldsymbol{y}_{0:t}, \boldsymbol{s}_{0:t}, \boldsymbol{\alpha}_{1:t}, \boldsymbol{\beta}_{1:t}, \boldsymbol{g}_{1:t}, \boldsymbol{\rho}_{1:t}, \boldsymbol{z}_{1:t}, \boldsymbol{m}_{1:t}) \\
&\quad \propto f(\boldsymbol{y}_0) f(\boldsymbol{s}_0) \prod_{t'=1}^{t} f(\boldsymbol{s}_{t'}|\boldsymbol{s}_{t'-1}) f(\underline{\boldsymbol{y}}_{t'}^{(1)}|\boldsymbol{y}_{t'-1}) f(\boldsymbol{g}_{t'}|\boldsymbol{s}_{t'}) f(\boldsymbol{\rho}_{t'}|\boldsymbol{s}_{t'}) \prod_{j=1}^{J} f(\bar{\boldsymbol{y}}_{t'}^{(j)}, \boldsymbol{\alpha}_{t'}^{(j)}, \boldsymbol{\beta}_{t'}^{(j)}, \boldsymbol{z}_{t'}^{(j)}, M_{t'}^{(j)}|\underline{\boldsymbol{y}}_{t'}^{(j)}, \boldsymbol{s}_{t'}) \\
&\quad \propto f(\boldsymbol{y}_0) f(\boldsymbol{s}_0) \prod_{t'=1}^{t} f(\boldsymbol{s}_{t'}|\boldsymbol{s}_{t'-1}) f(\underline{\boldsymbol{y}}_{t'}^{(1)}|\boldsymbol{y}_{t'-1}) f(\boldsymbol{g}_{t'}|\boldsymbol{s}_{t'}) f(\boldsymbol{\rho}_{t'}|\boldsymbol{s}_{t'})
\end{aligned}$$

4

$$\times \prod_{j=1}^{J} f\big(\boldsymbol{z}_{t'}^{(j)} \big| \bar{\boldsymbol{y}}_{t'}^{(j)}, \boldsymbol{\alpha}_{t'}^{(j)}, M_{t'}^{(j)}, \underline{\boldsymbol{y}}_{t'}^{(j)}, \boldsymbol{s}_{t'}\big) f\big(\bar{\boldsymbol{y}}_{t'}^{(j)}, \boldsymbol{\alpha}_{t'}^{(j)}, \boldsymbol{\beta}_{t'}^{(j)}, M_{t'}^{(j)} \big| \underline{\boldsymbol{y}}_{t'}^{(j)}, \boldsymbol{s}_{t'}\big) . \tag{7}$$

By further extending each terms of (7) accounting for the likelihood of measurements, the distinction between legacy and new PTs, and DA variables we have

$$\begin{aligned}
&f\big(\boldsymbol{y}_{0:t}, \boldsymbol{s}_{0:t}, \boldsymbol{\alpha}_{1:t}, \boldsymbol{\beta}_{1:t} \big| \boldsymbol{g}_{1:t}, \boldsymbol{\rho}_{1:t}, \boldsymbol{z}_{1:t}\big) \\
&\quad \propto f(\boldsymbol{y}_0) f(\boldsymbol{s}_0) \prod_{t'=1}^{t} \underbrace{\Bigg(\prod_{a\in\mathcal{V}} \tau\big(\boldsymbol{s}_{a,t'} \big| \boldsymbol{s}_{a,t'-1}\big) \Bigg)}_{\text{Vehicle Prediction}} \underbrace{\Bigg(\prod_{a\in\mathcal{V}_{t'}^{g}} \mathfrak{g}_a\big(\boldsymbol{g}_{a,t'} \big| \boldsymbol{s}_{a,t'}\big) \Bigg) \Bigg(\prod_{a\in\mathcal{R}} \prod_{a'\in\mathcal{T}_{t'}^{(a)}} \mathfrak{d}\big(\boldsymbol{\rho}_{t'}^{(a,a')} \big| \boldsymbol{s}_{a,t'}, \boldsymbol{s}_{a',t'}\big) \Bigg)}_{\text{CSL}} \\
&\quad \times \underbrace{\Bigg(\prod_{\ell\in\mathcal{L}_{t'}^{(1)}} f\big(\underline{\boldsymbol{y}}_{\ell,t'}^{(1)} \big| \boldsymbol{y}_{\ell,t'-1}\big) \Bigg)}_{\text{PT Prediction}} \prod_{j=1}^{J} \underbrace{\Bigg(\prod_{\ell\in\mathcal{L}_{t'}^{(j)}} q\big(\underline{\boldsymbol{y}}_{\ell,t'}^{(j)}, \alpha_{\ell,t'}^{(j)}, \boldsymbol{s}_{j_1,t'}, \boldsymbol{s}_{j_2,t'}; \boldsymbol{z}_{t'}^{(j)}\big) \prod_{m\in\mathcal{M}_{t'}^{(j)}} \psi\big(\alpha_{\ell,t'}^{(j)}, \beta_{m,t'}^{(j)}\big) \Bigg)}_{\text{MTT with DA}} \\
&\quad \times \underbrace{\Bigg(\prod_{a\in\mathcal{V}} h\big(\boldsymbol{s}_{a,t'}, \alpha_{L+a,t'}^{(j)}, \boldsymbol{s}_{j_1,t'}, \boldsymbol{s}_{j_2,t'}; \boldsymbol{z}_{t'}^{(j)}\big) \prod_{m\in\mathcal{M}_{t'}^{(j)}} \psi\big(\alpha_{L+a,t'}^{(j)}, \beta_{m,t'}^{(j)}\big) \Bigg) \prod_{m\in\mathcal{M}_{t'}^{(j)}} \upsilon\big(\bar{\boldsymbol{y}}_{m,t'}^{(j)}, \beta_{m,t'}^{(j)}, \boldsymbol{s}_{j_1,t'}, \boldsymbol{s}_{j_2,t'}; \boldsymbol{z}_{m,t'}^{(j)}\big)}_{\text{MTT with DA}} ,
\end{aligned} \tag{8}$$

where functions $q(\cdot)$, $\psi(\cdot)$, $h(\cdot)$ and $\upsilon(\cdot)$ are associated to legacy PTs, DA, vehicles, and new PTs, respectively; their expressions are provided in [23]. The factorization in (8) is related to a factor graph, which is the operating structure used to run the message passing algorithm in a sequential manner over the pairs $j \in \mathcal{J}$. We recall that the processing occurs in one fusion center (centralized architecture). We use standard rules for calculating messages and beliefs [13, 24], which are represented by particles [12, 13].

4 Numerical results

The proposed approach is general enough to be applied in different contexts and domains. Indeed, we first present a preliminary analysis in a simulated urban scenario with four moving land vehicles, followed by results with real data acquired by NATO CMRE in a maritime surveillance trial.

In the vehicular urban scenario (Fig. 1a) four moving vehicles use GNSS, inter-vehicle and MOT measurements to perform CSL and MTT of two static targets located in the middle of the area and appearing at time $t = 5$ s. GNSS accuracy is of 5 m, inter-vehicle and MOT measurements include range and bearing information with accuracy of 3 m and 1 deg, respectively.

The analysis focuses on the localization in case of GNSS unavailability: we induce an outage event (from $t = 15$ s to $t = 30$ s) with the aim to evaluate the robustness of the proposed methodology, which uses targets information to refine vehicles' positioning, compared to the case where CSL and MTT are performed as separate tasks, and target state estimates are not used as anchor points to improve the vehicles localization. The achieved results on vehicle localization accuracy are reported in Fig. 1b. We also report the optimal subpattern assignment (OSPA) in Fig. 1c and the time on target (Fig. 1d) for distance thresholds ranging from 1 m to 20 m.

The second scenario, instead, refers to a hybrid, autonomous, robotic network developed by NATO CMRE for maritime surveillance applications. The data we use was gathered during the littoral continuous active sonar trial conducted off the coast of Piombino, Italy, in November 2018 (LCAS18). The network consists of mobile and fixed gateways that constitute the communication infrastructure, and of autonomous underwater vehicles (AUVs), Harpo and Groucho, capable of detecting and tracking possible threats, and communicating the acquired data to the command and control (C2) center. The vehicles are classified as surface vehicles (towed sonar source, acoustic modems and waveglider) and underwater ones (AUVs) towing linear arrays of hydrophones for acoustic communications. GNSS navigation data are available for all the surface vehicles with an accuracy of 5 m, while

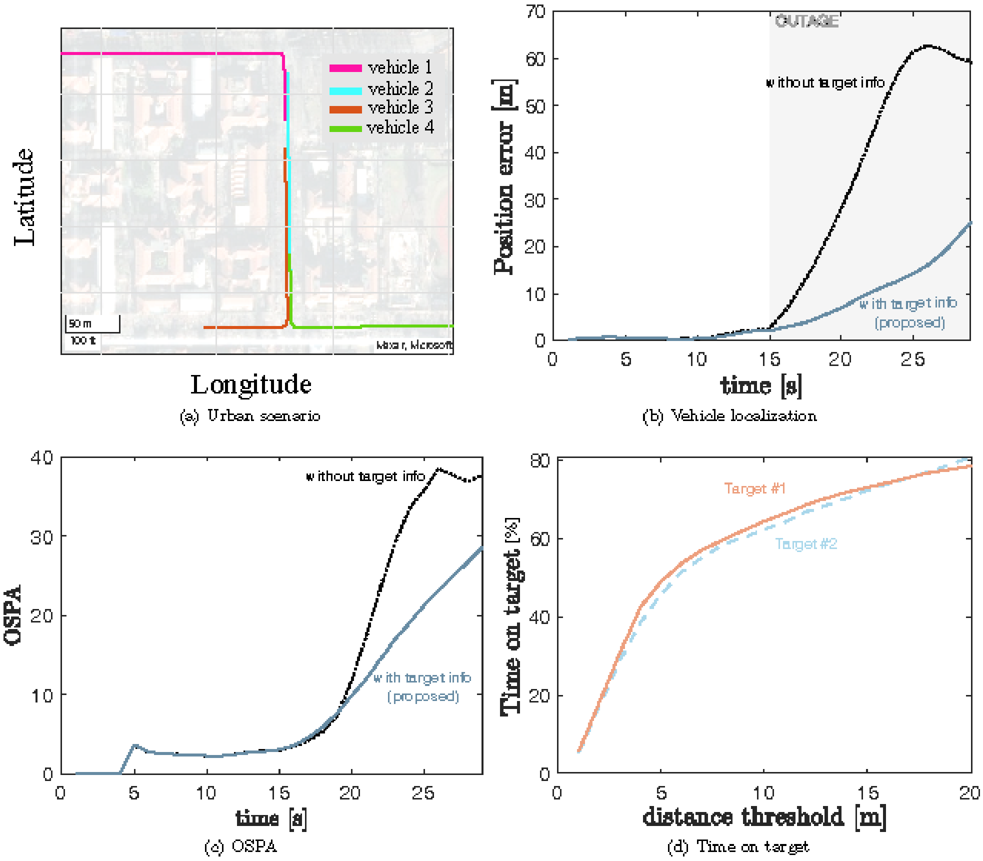

Figure 1: Results of vehicle localization in an urban scenario with a GNSS outage event. a) True trajectories of vehicles and position of static targets; b) vehicle localization error; c) OSPA metric; and d) time on target.

inter-vehicle and MOT measurements are of the form of range and bearing, with accuracy set to 70 m and 7 deg, respectively.

Fig. 2a shows the ground truth (black) and reconstructed (colored curves) trajectories by the proposed methodologies for moving vehicles and target, highlighting the fidelity in estimating their motion over a wide maritime area. Lastly, Fig. 2b presents the accuracy in localization of AUVs Groucho and Harpo, with average errors of 67.1 m and 50.9 m, respectively. We also report that the average error on target localization in this experiment has been of 279.4 m.

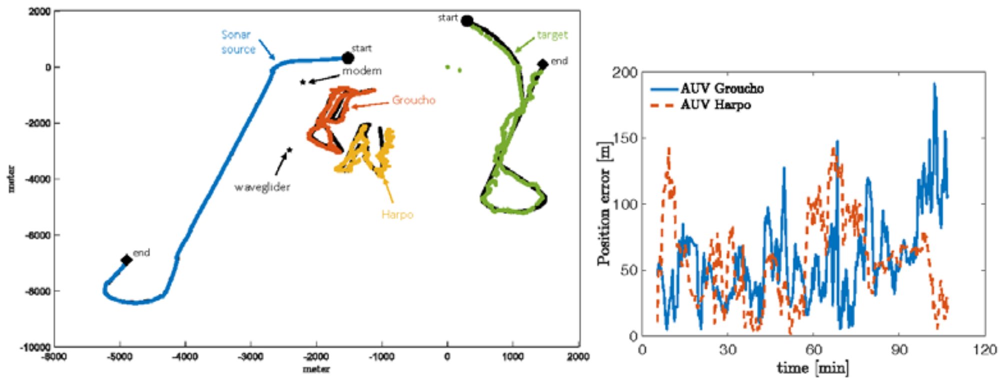

(a) Maritime scenarios with real (black) and estimated (colored) trajectories

(b) AUV localization

Figure 2: Results of vehicle localization in an maritime scenario. a) Scenario with true and estimated trajectories; and b) AUV localization error.

5 Conclusion

We addressed the problem of cooperative network localization and multitarget tracking in vehicular networks characterized by the mobility of the sensing devices. We designed a centralized algorithm based on belief propagation that integrates CSL and MTT tasks and exploits target beliefs to refine the CSL of sensing vehicles. Analysis in a simulated urban scenario as well as in a realistic underwater network demonstrates the feasibility and benefits of the proposed methodology.

References

[1] E. D. Kaplan and C. Hegarty, *Understanding GPS: Principles and Applications.* Norwood: Artech House, 2006.

[2] I. Akyildiz, W. Su, Y. Sankarasubramaniam, and E. Cayirci, "A survey on sensor networks," *IEEE Commun. Mag.*, vol. 40, pp. 102–114, Nov. 2002.

[3] F. Gustafsson and F. Gunnarsson, "Mobile positioning using wireless networks: possibilities and fundamental limitations based on available wireless network measurements," *IEEE Signal Process. Mag.*, vol. 22, pp. 41–53, Jun. 2005.

[4] N. Patwari, J. N. Ash, S. Kyperountas, A. O. Hero, R. L. Moses, and N. S. Correal, "Locating the nodes: Cooperative localization in wireless sensor networks," *IEEE Signal Process. Mag.*, vol. 22, pp. 54–69, Jul. 2005.

[5] H. Wymeersch, J. Lien, and M. Z. Win, "Cooperative localization in wireless networks," *Proc. IEEE*, vol. 97, pp. 427–450, Feb. 2009.

[6] M. Z. Win, A. Conti, S. Mazuelas, Y. Shen, W. M. Gifford, D. Dardari, and M. Chiani, "Network localization and navigation via cooperation," *IEEE Commun. Mag.*, vol. 49, pp. 56–62, May 2011.

[7] L. D. Xu, W. He, and S. Li, "Internet of things in industries: A survey," *IEEE Signal Process. Mag.*, vol. 10, pp. 2233–2243, Jan. 2014.

[8] M. Z. Win, Y. Shen, and W. Dai, "A theoretical foundation of network localization and navigation," *Proc. IEEE*, vol. 106, pp. 1136–1165, Jul. 2018.

[9] M. Brambilla, G. Soatti, and M. Nicoli, "Precise vehicle positioning by cooperative feature association and tracking in vehicular networks," in *2018 IEEE Statistical Signal Process. Workshop (SSP)*, pp. 648–652, Aug. 2018.

[10] F. Zafari, A. Gkelias, and K. K. Leung, "A survey of indoor localization systems and technologies," *Commun. Surveys Tuts.*, vol. 21, pp. 2568–2599, Apr. 2019.

[11] G. Ferri, A. Munafò, A. Tesei, P. Braca, F. Meyer, K. Pelekanakis, R. Petroccia, J. Alves, C. Strode, and K. LePage, "Cooperative robotic networks for underwater surveillance: An overview," *IET Radar, Sonar Navig.*, vol. 11, pp. 1740–1761, Dec. 2017.

[12] F. Meyer, P. Braca, P. Willett, and F. Hlawatsch, "A scalable algorithm for tracking an unknown number of targets using multiple sensors," *IEEE Trans. Signal Process.*, vol. 65, pp. 3478–3493, Jul. 2017.

[13] F. Meyer, T. Kropfreiter, J. L. Williams, R. Lau, F. Hlawatsch, P. Braca, and M. Z. Win, "Message passing algorithms for scalable multitarget tracking," *Proc. IEEE*, vol. 106, pp. 221–259, Feb. 2018.

[14] G. Soldi, F. Meyer, P. Braca, and F. Hlawatsch, "Self-tuning algorithms for multisensor-multitarget tracking using belief propagation," *IEEE Trans. Signal Process.*, vol. 67, pp. 3922–3937, Aug. 2019.

[15] G. Ferri, A. Munafó, and K. D. LePage, "An autonomous underwater vehicle data-driven control strategy for target tracking," *IEEE J. Ocean. Eng.*, vol. 43, pp. 323–343, Feb. 2018.

[16] F. Meyer, O. Hlinka, H. Wymeersch, E. Riegler, and F. Hlawatsch, "Distributed localization and tracking of mobile networks including noncooperative objects," *IEEE Trans. Signal Inf. Process. Netw.*, vol. 2, pp. 57–71, Mar. 2016.

[17] F. Meyer and M. Z. Win, "Joint navigation and multitarget tracking in networks," in *Proc. IEEE ICC-18*, (Kansas City, MO, USA), pp. 1–6, May 2018.

[18] P. Sharma, A. Saucan, D. J. Bucci, and P. K. Varshney, "Decentralized Gaussian filters for cooperative self-localization and multi-target tracking," *IEEE Trans. Signal Process.*, vol. 67, pp. 5896–5911, Nov. 2019.

[19] M. Brambilla, M. Nicoli, G. Soatti, and F. Deflorio, "Augmenting vehicle localization by cooperative sensing of the driving environment: Insight on data association in urban traffic scenarios," *IEEE Trans. Intell. Transp. Syst.*, vol. 21, pp. 1646–1663, Sep. 2020.

[20] R. Mendrzik, M. Brambilla, C. Allmann, M. Nicoli, W. Koch, G. Bauch, K. LePage, and P. Braca, "Joint multitarget tracking and dynamic network localization in the underwater domain," in *Proc. IEEE ICASSP-20*, (Barcelona, Spain), pp. 4890–4894, May 2020.

[21] D. Gaglione, G. Soldi, F. Meyer, F. Hlawatsch, P. Braca, A. Farina, and M. Z. Win, "Bayesian information fusion and multitarget tracking for maritime situational awareness," *IET Radar, Sonar Navig.*, vol. 14, pp. 1845–1857, Dec. 2020.

[22] D. Gaglione, G. Soldi, P. Braca, G. De Magistris, F. Meyer, and F. Hlawatsch, "Classification-aided multitarget tracking using the sum-product algorithm," *IEEE Signal Process. Letters*, vol. 27, pp. 1710–1714, Sep. 2020.

[23] M. Brambilla, D. Gaglione, G. Soldi, R. Mendrzik, G. Ferri, K. D. LePage, M. Nicoli, P. Willett, P. Braca, and M. Z. Win, "Cooperative localization and multitarget tracking in agent networks with the sum-product algorithm," 2021. https://arxiv.org/abs/2108.02573.

[24] F. R. Kschischang, B. J. Frey, and H.-A. Loeliger, "Factor graphs and the sum-product algorithm," *IEEE Trans. Inf. Theory*, vol. 47, pp. 498–519, Feb. 2001.